




## Optimizing through-space interaction for singlet fission by using macrocyclic structures†

Zhangxia Wang,<sup>a</sup> Xuexiao Yang,<sup>a</sup> Haibo Ma <sup>\*b</sup> and Xiaoyu Xie<sup>\*c</sup>Cite this: *J. Mater. Chem. C*, 2023, 11, 6856Received 28th March 2023,  
Accepted 1st May 2023

DOI: 10.1039/d3tc01077e

rsc.li/materials-c

There is great interest in the exploitation of singlet fission (SF) materials to improve the power conversion efficiency (PCE) of solar cells. Usually, ultrafast SF is achieved as an intermolecular process (xSF). However, it isn't easy to precisely tune crystal packing in the experiment. In contrast, electronic structural properties can be exactly tuned in intramolecular SF (iSF) materials by changing different linkers. Nevertheless, few designs can achieve ultrafast SF in iSF materials. In this work, we use macrocyclic structures to maintain the  $\pi$ - $\pi$  packing between two pentacenes and optimize through-space interaction in iSF. First, we conduct a detailed discussion on the experimentally discovered bipentacene macrocycle (BPC) and phenylene-linked bipentacene (BP1) by performing high-level electronic structure calculations and molecular dynamics (MD) sampling. The calculated iSF rates are in good agreement with experimental measurements. More importantly, the macrocyclic scaffold in BPC only plays a role in restricting the relative position of two pentacenes and does not affect the electronic coupling between excited states. Accordingly, 19 optimal structures are screened out from 97 initial candidates, and those 19 systems exhibit remarkably efficient iSF features with unprecedented ultrafast time constants (tens of femtoseconds).

## 1 Introduction

Singlet fission (SF) is a photophysical process typical of some organic compounds, where a high-energy singlet state splits into two low-energy triplet states. Compared with conventional semiconductor materials, SF materials generate two excitons

from one single absorbed photon, which can achieve photocurrent multiplication theoretically.<sup>1,2</sup> It has been demonstrated that sensitizing solar cells using singlet fission can reduce thermalization losses and improve light sensitivity.<sup>3–9</sup> To break the 45% power conversion efficiency limit of conventional photovoltaic devices,<sup>1</sup> scientists have devoted great efforts to unravelling the SF mechanisms<sup>10–17</sup> and discovering more effective SF materials.<sup>18–26</sup>

An efficient SF process requires sufficiently large electronic coupling between two chromophores in addition to satisfying the energy level matching conditions ( $E(S_1) \geq 2E(T_1)$  and  $E(T_2) \geq 2E(T_1)$ ).<sup>18</sup> Usually, electronic couplings originate from close packing between adjacent chromophores in intermolecular singlet fission (xSF, see in Fig. 1a). It is generally believed that slip-stacked packing is beneficial to singlet fission.<sup>21,27–30</sup> Wang *et al.* illustrated that slip-stacked packing could increase the SF rate by more than an order of magnitude compared to cofacial stacking of pentacene through nonadiabatic molecular dynamics calculations.<sup>29</sup> In both experiment and calculation work, people can modulate molecular packing and electronic properties by introducing either the heteroatom in the backbone or terminally halogenated modification,<sup>31–39</sup> changing the side groups<sup>40–45</sup> or adding spacer molecules between SF chromophores.<sup>46</sup> However, in crystalline media, photophysical processes depend not only on crystal packing but also on the influence of many other factors, such as crystallinity, morphology, and defects.<sup>47–53</sup> Despite creative endeavours in this regard, tuning electronic properties in the solid state is experimentally challenging because interchromophoric interaction is highly sensitive to slight changes in chromophore arrangement.

During the past decade, intramolecular singlet fission (iSF) has attracted many research interests because of its precise tunability of number, connectivity, and interchromophoric interactions.<sup>54–66</sup> Moreover, the iSF process can be easily tuned by changing the chemical composition of the linker (Fig. 1b). Since 2015, dimers,<sup>22,67,68</sup> oligomers<sup>69–74</sup> and polymers<sup>75</sup> of chromophore molecules (*e.g.*, acene or rylene) have been discovered for iSF. Among the chromophores, pentacene and tetracene are the most extensively studied because of their high

<sup>a</sup> School of Chemistry and Chemical Engineering, Nanjing University, Nanjing 210023, China<sup>b</sup> Qingdao Institute for Theoretical and Computational Sciences, Qingdao Institute of Frontier and Interdisciplinary Science, Shandong University, Qingdao 266237, China. E-mail: haibo.ma@sdu.edu.cn<sup>c</sup> Department of Chemistry, University of Liverpool, Liverpool L69 3BX, UK. E-mail: xiaoyu@liverpool.ac.uk† Electronic supplementary information (ESI) available. See DOI: <https://doi.org/10.1039/d3tc01077e>

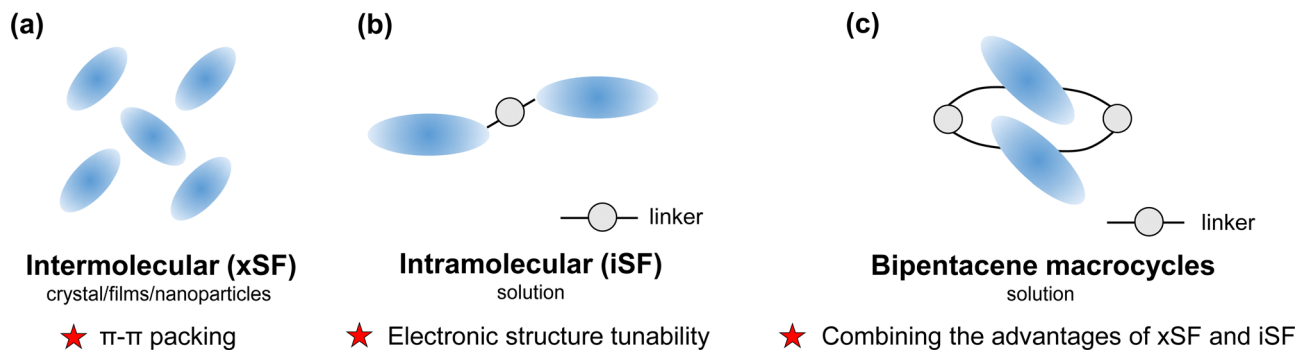


Fig. 1 Summary of characteristics in (a) intermolecular singlet fission (xSF) and (b) intramolecular singlet fission (iSF) and (c) the design strategy for bipentacene macrocycles.

charge mobility and well energy level matching for SF.<sup>18,76–78</sup> It has been recently reported that introducing different linkers between the two pentacenes can change singlet fission rates by orders of magnitude (from femtosecond to nanosecond).<sup>54,60,79</sup>

Can we take advantage of the molecular control inherent in iSF to help the challenging control of packing in xSF? (Fig. 1c). Are there other ways to achieve slip-stacked packing between chromophores? Over a half-century, the synthesis of structurally specific macrocycles has developed rapidly,<sup>80–82</sup> providing the possibility to synthesize chromophore-containing macrocycles. This idea was verified by Tilley's group in 2020.<sup>83</sup> They reported two types of pentacene-containing macrocycles: pentacene dimerized macrocycles, and pentacene trimerized macrocycles. The pentacene dimerized macrocycle (marked as 1b in their work) exhibits an ideal SF rate (13.8 ps) and triplet yield (170%) in chloroform solution. Similarly, Yoshizawa *et al.*<sup>84</sup> demonstrated that the macrocyclic framework facilitates the interaction between three adjacent pentacene units, resulting in efficient SF in solution. According to the SF behaviour brought by the structure specificity of macrocycles, it looks promising to design a variety of ideal SF materials.

Before designing bipentacene macrocycles, it is necessary to find out how iSF occurs in the macrocycles. There are two driving forces in iSF systems: through-space and through-bond interactions. It has been proved theoretically and experimentally that through-bond interactions play a crucial role for many bipentacenes, such as the well-known *ortho*-, *meta*- and *para*-pentacene dimers.<sup>56,85</sup> For *ortho*-pentacene dimers, the calculated total coupling is 16.4 meV, and the coupling of the through-space model is 1.57 meV (about 10% of the total one).<sup>86</sup> Furthermore, the through-space interactions dominate the iSF process in some covalently bridged bipentacenes with unique spatial proximity of the two pentacenes.<sup>60,79,87–90</sup> According to previous experimental and theoretical experience on bipentacenes, we speculate that the through-space interactions of the bipentacene macrocycles are the key factor in the occurrence of iSF, but is it the dominant factor? In addition to the role of structural confinement mentioned in the experiment, does the rigid scaffold have other functions? These issues need to be adequately addressed before designing bipentacene macrocycles.

In this work, we present an accurate quantitative study for clarifying the above mechanism controversial issues in iSF with

macrocyclic structures by taking the experimentally discovered bipentacene macrocycle and phenylene-linked bipentacene (see Fig. 2). Our calculations combining high-level electronic structure calculations, molecular dynamics (MD) sampling, and Fermi golden rule achieve good agreement with experimental measurements for iSF rates. We find the macrocyclic structure can maintain the optimal π-π stacking of two pentacenes in solution. Furthermore, based on these new findings, we suggest 97 macrocyclic scaffolds with different lengths to help the two pentacene units optimize their packing structure. Then 19 optimal structures are screened out from these 97 candidates, and the detailed quantum chemical calculations reveal that these systems can exhibit remarkably efficient iSF features with ultrafast time constants of unprecedented tens of femtoseconds. The work presented here opens a new scenario for designing new molecules to improve the singlet fission efficiency by combining the advantages of both close π-π stacking in xSF and chemical diversity in iSF.

## 2 Methodologies and computational details

### 2.1 Model systems

To explore the mechanism of BPc singlet fission, we adopt the molecules in Fig. 2 as our model systems. The phenylene-linked



Fig. 2 Model molecules studied in this work. BPc is used to model 1b studied in ref. 83, and BP1 is used to model the same molecule studied in ref. 54. BPc-1 and BP1-1 are the corresponding truncated models.





where

$$f_e(E) = \frac{\rho_e(E)}{\int_{-\infty}^{\infty} dE \rho_e(E)}, \quad (6)$$

and

$$f_a(E) = \frac{\rho_a(E)}{\int_{-\infty}^{\infty} dE \rho_a(E)}. \quad (7)$$

Here,  $\rho_e(E)$  and  $\rho_a(E)$  are the unnormalized density of states involved in an emission  $S_1 \rightarrow T_1$  spectra and absorption  $S_0 \rightarrow T_1$  spectra which can be calculated by:

$$\rho_{\text{e/a}}(E) = \sum_n^{\infty} \frac{S^n}{n!} \exp \left[ -4 \ln 2 \left( \frac{E - E_0 \pm n \hbar \omega}{\text{fwhm}} \right)^2 \right]. \quad (8)$$

In eqn (8), the emission process (e) takes a positive sign, and the absorption (a) process takes a negative sign.  $E_0$  is the 0-0 transition energy and  $\omega$  is the frequency of the effective high-frequency mode. The full width at half-maximum (fwhm) is used

to account for the effects of all other modes and solvent effects.  $S$  is the HuangRhys factor calculated using the reorganization energy  $\lambda$ :  $S = \lambda/\hbar\omega$ .

In this work,  $E_0$ ,  $\omega$  and fwhm are extracted from experimental absorption spectra of the monomeric model compound for BP1 (TIPS pentacene) and BPc (pentacene). Reorganization energy  $\lambda$  is calculated by time-dependent DFT (TDDFT) with Tamm–Dancoff approximations (TDA) at B3LYP/6-31G(d) level. All parameters are listed in Table S1 (ESI<sup>†</sup>).

Since the experiment gaps between LE and TT states are applied for the FCWD and rate calculation,  $V_{\text{eff1}}$  and  $V_{\text{eff2}}$  would not be distinguished in practice in a specific snapshot based on the QC calculation, and they are averaged to compute the final  $|V|^2$ .

### 3 Results and discussion

### 3.1 Through-space/through-bond interaction

Singlet fission systems have two driving forces: through-space and through-bond interactions. The through-space situation means that two chromophores have spatial orbital overlap due to the special close packing. In contrast, through-bond means that the linker orbitals are strongly coupled to both chromophores, enhancing the effective interaction between chromophores. In order to explore the driving force of bipentacenes, we take BPc and BP1 as our model systems, where BP1 is the representative of the through-bond iSF system.

First, we calculate the electronic Hamiltonian of BPC, BP1 and their corresponding through-space systems (BPC-1 and BP1-1) at equilibrium molecular geometries. As shown in Fig. 3a, all electronic couplings (absolute values) are close in BPC and BPC-1, indicating that the presence or absence of a macrocyclic scaffold does not affect the coupling between electronic states. The through-space interaction dominates the iSF process in BPC. Moreover, Hamiltonian elements (the full Hamiltonian can be found in ESI<sup>†</sup>) are similar to references' works in xSF systems. *E.g.*, coupling terms<sup>29,99</sup> and energy gap between LE and TT state (around 0.35–0.55 eV) compared to experimental results<sup>106,107</sup> (0.47 eV), suggesting that the linker weakly affects the electronic

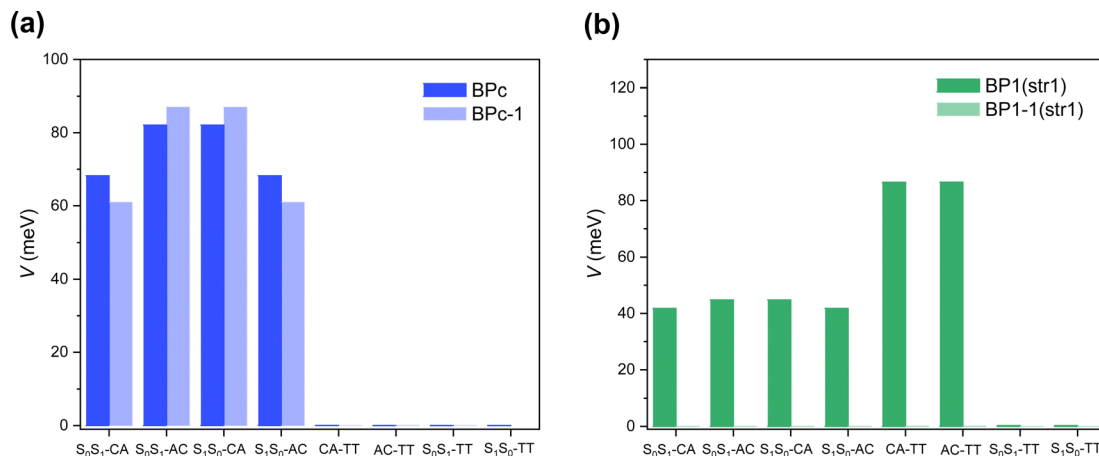


**Fig. 3** Electronic couplings (absolute values) between different diabatic states at equilibrium structures of (a) BPc and (b) BP1.



Second, we perform MD simulations to capture the effect of electronic couplings fluctuation for the reason that BPC and BP1 have large flexibility in the solution environment. The calculated effective electronic couplings of 10 samples are shown in Fig. 4.

**Table 1** Effective electronic couplings ( $|V_{\text{eff}}|^2$ ), FCWD terms and time constants ( $\tau$ ) of singlet fission in bipentacene systems. ( $|V_{\text{eff}}|_{\text{eq}}^2$  is the effective electronic couplings at equilibrium structures;  $|V_{\text{eff}}|_{10}^2$  is the average effective electronic couplings at 10 molecular dynamics snapshots)

System	$ V_{\text{eff}} _{\text{eq}}^2$ (meV <sup>2</sup> )	$ V_{\text{eff}} _{10}^2$ (meV <sup>2</sup> )	FCWD (eV <sup>-1</sup> )	$\tau_{\text{cal}}$ (ps)	$\tau_{\text{exp}}$ (ps)
BPc	0.00	10.41	0.980	10.3	13.8 (ref. 83)
BP1	0.18	0.21	2.162	228.8	20.0 (ref. 54)

We can find that couplings between different samples change over two orders of magnitude in both systems, reflecting that the influence of thermal fluctuation on the SF rate also exceeds two orders of magnitude. Therefore, we take the effective coupling average of 10 samples, and the calculated SF rates achieve an unprecedented good agreement with the experimental values (Table 1). Compared to BP1, BPc undergoes faster singlet fission (the calculated time constants of BPc and BP1 are 10.3 ps and 228.8 ps, respectively). Similar to the results under the static structure, the macrocyclic scaffolds keep two pentacenes persistent  $\pi$ - $\pi$  packing in MD, leading to singlet fission through spatial coupling in BPc.

### 3.2 Expanding the chemical space

Since only BPc has been found experimentally on bipentacene macrocycles, we try to get more ideal bipentacene materials through theoretical simulation. Based on the above findings, we change the macrocyclic scaffold to achieve  $\pi$ - $\pi$  stacking of two pentacenes, which is similar to BPc. Because the linker plays the role of structural support in the iSF process, its choice will be numerous for both conjugated and unconjugated ones. Moreover, the slipped distance between pentacenes will be easily regulated by linkers of different lengths.

To construct bipentacene macrocyclic scaffolds, we explore a large number of macrocyclic molecules discovered in recent

experiments,<sup>111–116</sup> as shown in the most left column of molecules in Fig. S8 (ESI<sup>†</sup>), where we select 25 existing linkers.  $H$ ,  $L$ ,  $T$  represent the slipped distances between the centre of mass of two pentacenes along the vertical, longitudinal and transverse axes, respectively (Fig. 5a). Among these bipentacene structures, except for a few molecules (43, 69, 73, 82, and 87 in Fig. S8, ESI<sup>†</sup>), the rest molecules have almost no displacement along the transverse axis due to the short and symmetric linkers. The relationship between xSF efficiency in pentacene dimers and the longitudinal and transverse displacements of the molecular backbones have been unravelled by Wang *et al.*<sup>29</sup> upon self-consistent fewest switches surface hopping (SC-FSSH) non-adiabatic simulations in conjunction with *ab initio* and semiempirical electronic structure calculations. They pointed out that the xSF rate can be increased by more than an order of magnitude by tuning the intermolecular packing, especially in the slipped stacked configurations with a shift of one ring along the transverse direction and an offset of one or two rings along the longitudinal axis are superior for SF (the local regions indicated by I, II, III and IV showed in Fig. 5b). The V and VI regions have the large CT character of the photoexcited state, which is found to be not essential for efficient SF.

Following Wang *et al.*'s suggestion<sup>29</sup> on slipping along the transverse direction about 2 Å to produce ultrafast xSF, we modify the experimentally existing linkers by enlarging conjugated length (*e.g.*, molecule 6 compared to 5 in Fig. S8, ESI<sup>†</sup>) or introducing asymmetric structures, (*e.g.*, 7, 8 compared to 5 in Fig. S8, ESI<sup>†</sup>), and 97 candidate molecules are designed finally. Then we perform structure optimization of these molecules in chloroform solvent by the computational method given in Section 2.1. There are five molecules (1, 2, 3, 86, and 91 in Fig. S8, ESI<sup>†</sup>) whose distances in the vertical direction exceed 4 Å, and the remaining 92 molecules, regardless of the length of the linker, maintain  $H$  at about 3.5 Å under the  $\pi$ - $\pi$  interaction of two pentacenes. Furthermore, the two pentacenes in 1, 2 and

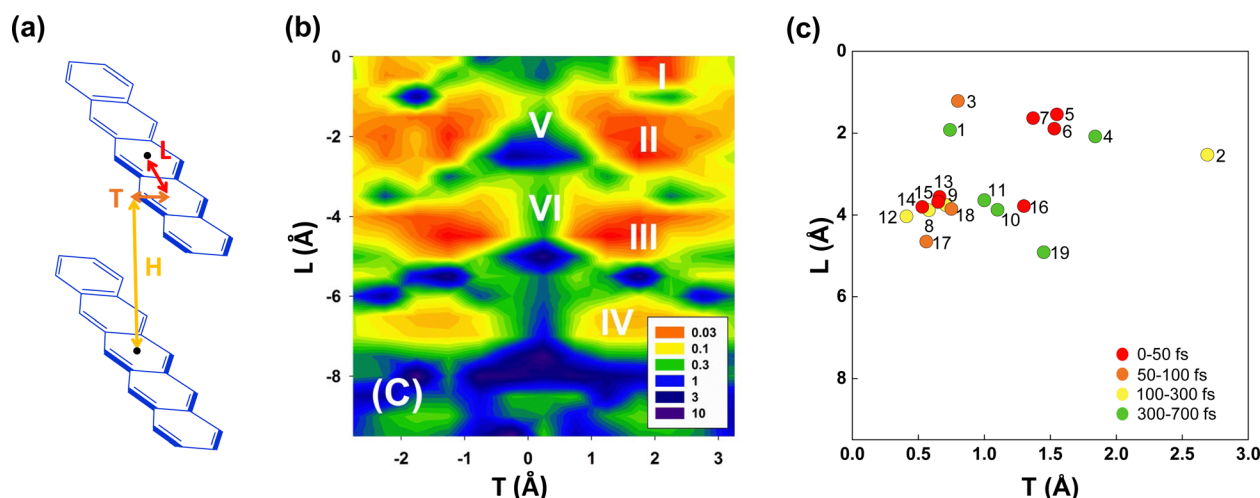


**Fig. 5** (a) Model molecular packing in designed bipentacene macrocycles.  $H$ ,  $L$  and  $T$  are the slipped distances between the centre of mass of the two pentacenes along the vertical, longitudinal and transverse axes, respectively. (b) Relationship between SF time constant (in ps) and pentacene slipped distances ( $H = 3.4$  Å). Reproduced with permission.<sup>29</sup> Copyright 2014, American Chemical Society. (c) Calculated SF time constants of 19 screened bipentacene macrocycles.

The bipentacene macrocycle consists of three parts: two pentacenes, two conjugated/covalent centres, and two legs connected to one conjugated/covalent centre (a total of four legs in one molecule). From the perspective of macrocycle selection, we give the following design recommendations:

Figure 1 displays the chemical structures and dimensions (H, L, T) for 17 phthalocyanine-based macrocyclic compounds (BPc1-BPc17). The structures are arranged in three rows, with dimensions listed below each structure.

Compound	H (Å)	L (Å)	T (Å)
BPc1	4.34	1.92	0.74
BPc2	3.57	2.53	2.69
BPc3	3.98	1.21	0.80
BPc4	3.66	2.08	1.84
BPc5	3.43	1.54	1.55
BPc6	3.39	1.89	1.53
BPc7	3.42	1.63	1.37
BPc8	3.50	3.88	0.58
BPc9	3.39	3.76	0.71
BPc10	3.39	3.87	1.10
BPc11	3.43	3.64	1.00
BPc12	3.53	4.03	0.41
BPc13	3.36	3.56	0.66
BPc14	3.42	3.80	0.53
BPc15	3.40	3.68	0.65
BPc16	3.44	3.78	1.30
BPc17	3.57	4.65	0.56
BPc18	3.44	3.85	0.75
BPc19	3.51	4.91	1.45

This journal is © The Royal Society of Chemistry 2023

Here, we constrain partial degrees of freedom in bipentacene *via* a macrocyclic structure. Compared to the conventional iSF system, the macrocycle enforces two chromophore units to be face-to-face ( $\pi$ - $\pi$  packing) by using two linkers instead of one along the transverse axis. Consequently, there are strong through-space interactions for singlet fission. Two linkers along the longitudinal axis can also be considered in the future. Unlike crystalline structures, the restriction using linkers is much more controllable. For example, the appropriate choice of the length of legs ensures the strong  $\pi$ - $\pi$  interaction and suitable displacement along the longitudinal and transverse axes. The introduction of asymmetric legs provides static displacement-shift along the transverse axis if the degree of freedom along transverse axes is controlled (as shown in our case), even if the thermal effect is not considered.

Based on the electronic structure analysis, the macrocyclic model is proven to be a good framework for iSF molecule design since the distance between chromophores can be highly controlled by its linker and the linker does not involve the electronic structure for SF. Therefore, design rules for packing xSF material can be used for the designing and preliminary searching of novel macrocyclic iSF molecules. Furthermore, an approach to calculating the SF rate is performed based on the Fermi golden rule and the rates of candidates are evaluated to conform to the high efficiency of these candidates.

Though our computational exploration is limited to 97 bipentacene macrocycles, their wide tunability is demonstrated. Our preliminary calculations on alternative linkers indicate that the same principles can be readily applied to similar materials systems. For example, two linkers can be connected longitudinally, pentacene can be replaced with other chromophores such as tetracene, and various linkers can be selected.

In addition, we find the macrocyclic structure maintains the ideal  $\pi$ - $\pi$  stacking of two pentacenes in solution and promotes the occurrence of ultrafast intramolecular singlet fission. Based on the aforementioned ideas, we design 97 candidate macrocyclic scaffolds, from which 19 promising new bipentacene macrocycles are proposed. The designed 19 materials display potential singlet fission and exhibited a superior iSF rate (fs). Here, we provide a novel design idea to optimize through-space interaction for intramolecular singlet fission using macrocyclic structures. Incorporating two pentacenes into a macrocycle is undoubtedly a good idea for iSF molecule design and can inspire more material discoveries.

H. M. and X. X. conceived the project. Z. W. designed the molecules and carried out the calculations. X. Y. and X. X. helped with the calculation process and provided inspiring suggestions for improvement. All the authors contributed to the data analysis and writing of the paper.

There are no conflicts to declare.

This work was supported by the National Key Research and Development Program of China (2022YFA1503103) and the National Natural Science Foundation of China (grant no. 22073045).

- 1 M. Hanna and A. Nozik, *J. Appl. Phys.*, 2006, **100**, 074510.
- 2 A. Rao and R. H. Friend, *Nat. Rev. Mater.*, 2017, **2**, 1–12.
- 3 D. N. Congreve, J. Lee, N. J. Thompson, E. Hontz, S. R. Yost, P. D. Reuswig, M. E. Bahlke, S. Reineke, T. Van Voorhis and M. A. Baldo, *Science*, 2013, **340**, 334–337.
- 4 M. Einzinger, T. Wu, J. F. Kompalla, H. L. Smith, C. F. Perkinson, L. Nienhaus, S. Wiegbold, D. N. Congreve, A. Kahn and M. G. Bawendi, *et al.*, *Nature*, 2019, **571**, 90–94.
- 5 L. Yang, M. Tabachnyk, S. L. Bayliss, M. L. Bohm, K. Broch, N. C. Greenham, R. H. Friend and B. Ehrler, *Nano Lett.*, 2015, **15**, 354–358.
- 6 J. Lee, P. Jadhav, P. D. Reuswig, S. R. Yost, N. J. Thompson, D. N. Congreve, E. Hontz, T. Van Voorhis and M. A. Baldo, *Acc. Chem. Res.*, 2013, **46**, 1300–1311.
- 7 J. Xia, S. N. Sanders, W. Cheng, J. Z. Low, J. Liu, L. M. Campos and T. Sun, *Adv. Mater.*, 2017, **29**, 1601652.
- 8 R. W. MacQueen, M. Liebhaber, J. Niederhausen, M. Mews, C. Gersmann, S. Jäckle, K. Jäger, M. J. Tayebjee, T. W. Schmidt and B. Rech, *et al.*, *Mater. Horiz.*, 2018, **5**, 1065–1075.
- 9 X. Qiao and D. Ma, *Mater. Sci. Eng., R*, 2020, **139**, 100519.



- 10 W.-L. Chan, T. C. Berkelbach, M. R. Provorse, N. R. Monahan, J. R. Tritsch, M. S. Hybertsen, D. R. Reichman, J. Gao and X.-Y. Zhu, *Acc. Chem. Res.*, 2013, **46**, 1321–1329.
- 11 K. Miyata, F. S. Conrad-Burton, F. L. Geyer and X.-Y. Zhu, *Chem. Rev.*, 2019, **119**, 4261–4292.
- 12 D. Casanova, *Chem. Rev.*, 2018, **118**, 7164–7207.
- 13 R. M. Young and M. R. Wasielewski, *Acc. Chem. Res.*, 2020, **53**, 1957–1968.
- 14 Y. Yao, *Phys. Rev. B*, 2016, **93**, 115426.
- 15 K.-W. Sun and Y. Yao, *J. Chem. Phys.*, 2017, **147**, 224905.
- 16 L. Xue, X. Song, Y. Feng, S. Cheng, G. Lu and Y. Bu, *J. Am. Chem. Soc.*, 2020, **142**, 17469–17479.
- 17 L. Wang, T.-S. Zhang, L. Fu, S. Xie, Y. Wu, G. Cui, W.-H. Fang, J. Yao and H. Fu, *J. Am. Chem. Soc.*, 2021, **143**, 5691–5697.
- 18 M. B. Smith and J. Michl, *Chem. Rev.*, 2010, **110**, 6891–6936.
- 19 M. B. Smith and J. Michl, *Annu. Rev. Phys. Chem.*, 2013, **64**, 361–386.
- 20 J. C. Johnson, A. J. Nozik and J. Michl, *Acc. Chem. Res.*, 2013, **46**, 1290–1299.
- 21 S. Ito, T. Nagami and M. Nakano, *J. Photochem. Photobiol., C*, 2018, **34**, 85–120.
- 22 T. Hasobe, S. Nakamura, N. V. Tkachenko and Y. Kobori, *ACS Energy Lett.*, 2021, **7**, 390–400.
- 23 Ö. H. Omar, D. Padula and A. Troisi, *ChemPhotoChem*, 2020, **4**, 5223–5229.
- 24 J. Wen, Z. Havlas and J. Michl, *J. Am. Chem. Soc.*, 2015, **137**, 165–172.
- 25 D. Padula, Ö. H. Omar, T. Nematiram and A. Troisi, *Energy Environ. Sci.*, 2019, **12**, 2412–2416.
- 26 T. Nagami, R. Sugimori, R. Sakai, K. Okada and M. Nakano, *J. Phys. Chem. A*, 2021, **125**, 3257–3267.
- 27 H. Miyamoto, K. Okada, K. Tokuyama and M. Nakano, *J. Phys. Chem. A*, 2021, **125**, 5585–5600.
- 28 E. A. Buchanan and J. Michl, *J. Am. Chem. Soc.*, 2017, **139**, 15572–15575.
- 29 L. Wang, Y. Olivier, O. V. Prezhdo and D. Beljonne, *J. Phys. Chem. Lett.*, 2014, **5**, 3345–3353.
- 30 S. Ito, T. Nagami and M. Nakano, *Phys. Chem. Chem. Phys.*, 2017, **19**, 5737–5745.
- 31 Y.-D. Zhang, Y. Wu, Y. Xu, Q. Wang, K. Liu, J.-W. Chen, J.-J. Cao, C. Zhang, H. Fu and H.-L. Zhang, *J. Am. Chem. Soc.*, 2016, **138**, 6739–6745.
- 32 N. Alagna, J. Han, N. Wollscheid, J. L. Perez Lustres, J. Herz, S. Hahn, S. Koser, F. Paulus, U. H. Bunz and A. Dreuw, *J. Am. Chem. Soc.*, 2019, **141**, 8834–8845.
- 33 T. Geiger, S. Schundelmeier, T. Hummel, M. Ströbele, W. Leis, M. Seitz, C. Zeiser, L. Moretti, M. Maiuri and G. Cerullo, *Chem. – Eur. J.*, 2020, **26**, 3420–3434.
- 34 C. Zeiser, L. Moretti, T. Geiger, L. Kalix, A. M. Valencia, M. Maiuri, C. Cocchi, H. F. Bettinger, G. Cerullo and K. Broch, *J. Phys. Chem. Lett.*, 2021, **12**, 7453–7458.
- 35 Y. Wu, K. Liu, H. Liu, Y. Zhang, H. Zhang, J. Yao and H. Fu, *J. Phys. Chem. Lett.*, 2014, **5**, 3451–3455.
- 36 R. D. Pensack, E. E. Ostroumov, A. J. Tilley, S. Mazza, C. Grieco, K. J. Thorley, J. B. Asbury, D. S. Seferos, J. E. Anthony and G. D. Scholes, *J. Phys. Chem. Lett.*, 2016, **7**, 2370–2375.
- 37 Y.-Y. Liu, C.-L. Song, W.-J. Zeng, K.-G. Zhou, Z.-F. Shi, C.-B. Ma, F. Yang, H.-L. Zhang and X. Gong, *J. Am. Chem. Soc.*, 2010, **132**, 16349–16351.
- 38 J. Herz, T. Buckup, F. Paulus, J. Engelhart, U. H. Bunz and M. Motzkus, *J. Phys. Chem. Lett.*, 2014, **5**, 2425–2430.
- 39 K. Bhattacharyya and A. Datta, *J. Phys. Chem. C*, 2019, **123**, 19257–19268.
- 40 C. Sutton, N. R. Tummala, D. Beljonne and J.-L. Bredas, *Chem. Mater.*, 2017, **29**, 2777–2787.
- 41 Z. Tang, S. Zhou, H. Liu, X. Wang, S. Liu, L. Shen, X. Lu and X. Li, *Mater. Chem. Front.*, 2020, **4**, 2113–2125.
- 42 K. Bhattacharyya and A. Datta, *J. Phys. Chem. C*, 2017, **121**, 1412–1420.
- 43 R. D. Pensack, A. J. Tilley, C. Grieco, G. E. Purdum, E. E. Ostroumov, D. B. Granger, D. G. Oblinsky, J. C. Dean, G. S. Doucette and J. B. Asbury, *et al.*, *Chem. Sci.*, 2018, **9**, 6240–6259.
- 44 C. Cao, G.-X. Yang, J.-H. Tan, D. Shen, W.-C. Chen, J.-X. Chen, J.-L. Liang, Z.-L. Zhu, S.-H. Liu and Q.-X. Tong, *et al.*, *Mater. Today Energy*, 2021, **21**, 100727.
- 45 A. K. Pal, K. Bhattacharyya and A. Datta, *J. Chem. Theory Comput.*, 2019, **15**, 5014–5023.
- 46 K. Broch, J. Dieterle, F. Branchi, N. Hestand, Y. Olivier, H. Tamura, C. Cruz, V. Nichols, A. Hinderhofer and D. Beljonne, *et al.*, *Nat. Commun.*, 2018, **9**, 1–9.
- 47 S. R. Yost, J. Lee, M. W. Wilson, T. Wu, D. P. McMahon, R. R. Parkhurst, N. J. Thompson, D. N. Congreve, A. Rao and K. Johnson, *et al.*, *Nat. Chem.*, 2014, **6**, 492–497.
- 48 G. B. Piland and C. J. Bardeen, *J. Phys. Chem. Lett.*, 2015, **6**, 1841–1846.
- 49 R. D. Pensack, A. J. Tilley, S. R. Parkin, T. S. Lee, M. M. Payne, D. Gao, A. A. Jahnke, D. G. Oblinsky, P.-F. Li and J. E. Anthony, *et al.*, *J. Am. Chem. Soc.*, 2015, **137**, 6790–6803.
- 50 S. T. Roberts, R. E. McAnally, J. N. Mastron, D. H. Webber, M. T. Whited, R. L. Brutchey, M. E. Thompson and S. E. Bradforth, *J. Am. Chem. Soc.*, 2012, **134**, 6388–6400.
- 51 J. N. Mastron, S. T. Roberts, R. E. McAnally, M. E. Thompson and S. E. Bradforth, *J. Phys. Chem. B*, 2013, **117**, 15519–15526.
- 52 D. Lubert-Perquel, E. Salvadori, M. Dyson, P. N. Stavrinou, R. Montis, H. Nagashima, Y. Kobori, S. Heutz and C. W. Kay, *Nat. Commun.*, 2018, **9**, 1–10.
- 53 M. L. Williams, I. Schlesinger, C. E. Ramirez, R. M. Jacobberger, P. J. Brown, R. M. Young and M. R. Wasielewski, *J. Phys. Chem. C*, 2022, **126**, 10287–10297.
- 54 S. N. Sanders, E. Kumarasamy, A. B. Pun, M. T. Trinh, B. Choi, J. Xia, E. J. Taffet, J. Z. Low, J. R. Miller and X. Roy, *et al.*, *J. Am. Chem. Soc.*, 2015, **137**, 8965–8972.
- 55 S. Lukman, A. J. Musser, K. Chen, S. Athanasopoulos, C. K. Yong, Z. Zeng, Q. Ye, C. Chi, J. M. Hodgkiss and J. Wu, *et al.*, *Adv. Funct. Mater.*, 2015, **25**, 5452–5461.
- 56 J. Zirzmeier, D. Lehnher, P. B. Coto, E. T. Chernick, R. Casillas, B. S. Basel, M. Thoss, R. R. Tykwinski and D. M. Guldi, *Proc. Natl. Acad. Sci. U. S. A.*, 2015, **112**, 5325–5330.



- Open Access Article. Published on 02/20/2023. Downloaded on 02/20/2023 13:07:45.  
This article is licensed under a Creative Commons Attribution 3.0 Unported Licence.



- 96 N. Monahan and X.-Y. Zhu, *Annu. Rev. Phys. Chem.*, 2015, **66**, 601–618.
- 97 B. S. Basel, J. Zirzmeier, C. Hetzer, S. R. Reddy, B. T. Phelan, M. D. Krzyaniak, M. K. Volland, P. B. Coto, R. M. Young and T. Clark, *et al.*, *Chem*, 2018, **4**, 1092–1111.
- 98 S. Lukman, K. Chen, J. M. Hodgkiss, D. H. Turban, N. D. Hine, S. Dong, J. Wu, N. C. Greenham and A. J. Musser, *Nat. Commun.*, 2016, **7**, 1–13.
- 99 X. Xie and A. Troisi, *J. Chem. Theory Comput.*, 2021, **18**, 394–405.
- 100 I. Fdez Galvan, M. Vacher, A. Alavi, C. Angeli, F. Aquilante, J. Autschbach, J. J. Bao, S. I. Bokarev, N. A. Bogdanov and R. K. Carlson, *et al.*, *J. Chem. Theory Comput.*, 2019, **15**, 5925–5964.
- 101 C. E. Miller, M. R. Wasielewski and G. C. Schatz, *J. Phys. Chem. C*, 2017, **121**, 10345–10350.
- 102 A. Montoya-Castillo, T. C. Berkelbach and D. R. Reichman, *J. Chem. Phys.*, 2015, **143**, 194108.
- 103 BIOVIA, Dassault Systèmes, *BIOVIA Materials Studio*, version: 2019, San Diego: Dassault Systèmes, 2019.
- 104 A. K. Rappé, C. J. Casewit, K. Colwell, W. A. Goddard III and W. M. Skiff, *J. Am. Chem. Soc.*, 1992, **114**, 10024–10035.
- 105 Z.-Q. You and C.-P. Hsu, *J. Phys. Chem. A*, 2011, **115**, 4092–4100.
- 106 E. Heinecke, D. Hartmann, R. Müller and A. Hese, *J. Chem. Phys.*, 1998, **109**, 906–911.
- 107 D. Smith, S. Tretiak, R. Martin, X. Chi, B. Crone, A. Ramirez and A. Taylor, *Phys. Rev. Lett.*, 2009, **102**, 017401.
- 108 H. Tamura, M. Huix-Rotllant, I. Burghardt, Y. Olivier and D. Beljonne, *Phys. Rev. Lett.*, 2015, **115**, 107401.
- 109 K. Miyata, Y. Kurashige, K. Watanabe, T. Sugimoto, S. Takahashi, S. Tanaka, J. Takeya, T. Yanai and Y. Matsumoto, *Nat. Chem.*, 2017, **9**, 983–989.
- 110 X. Xie, A. Santana-Bonilla, W. Fang, C. Liu, A. Troisi and H. Ma, *J. Chem. Theory Comput.*, 2019, **15**, 3721–3729.
- 111 K. Miki and K. Ohe, *Eur. J. Chem.*, 2020, **26**, 2529–2575.
- 112 Q. Shi, X. Wang, B. Liu, P. Qiao, J. Li and L. Wang, *Chem. Commun.*, 2021, **57**, 12379–12405.
- 113 J. J. Christensen, D. J. Eatough and R. M. Izatt, *Chem. Rev.*, 1974, **74**, 351–384.
- 114 S. Toyota, *Chem. Rev.*, 2010, **110**, 5398–5424.
- 115 M. Iyoda, J. Yamakawa and M. J. Rahman, *Angew. Chem., Int. Ed.*, 2011, **50**, 10522–10553.
- 116 M. A. Majewski and M. Stepień, *Angew. Chem., Int. Ed.*, 2019, **58**, 86–116.
- 117 T. C. Berkelbach, M. S. Hybertsen and D. R. Reichman, *J. Chem. Phys.*, 2014, **141**, 074705.

